Conformation Transition in Silk Protein Films Monitored by Time-Resolved Fourier Transform Infrared Spectroscopy: Effect of Potassium Ions on *Nephila* Spidroin Films†

Xin Chen,*,‡,§ David P. Knight,§ Zhengzhong Shao,‡ and Fritz Vollrath§

Department of Macromolecular Science, The Key Laboratory of Molecular Engineering of Polymers of Education Ministry, Fudan University, Shanghai 200433, People's Republic of China, and Department of Zoology, University of Oxford, South Parks Road, Oxford OX1 3PS, U.K.

Received July 31, 2002; Revised Manuscript Received October 16, 2002

ABSTRACT: We used time-resolved Fourier transform infrared spectroscopy (FTIR) to follow a conformation transition in *Nephila* spidroin film from random coil and/or helical structures to β-sheet induced by the addition of KCl from 0.01 to 1.0 mol/L in D_2O. Time series difference spectra showed parallel increases in absorption at 1620 and 1691 cm^{-1}, indicating formation of β-sheet, together with a coincident loss of intensity of ~1650 cm^{-1}, indicating decrease of random coil and/or helical structures. Increase in KCl concentration produced an increased rate of the conformation transition that may attributable to weakening of hydrogen bonds within spidroin macromolecules. The conformation transition was a biphasic process with [KCl] ≥ 0.3 mol/L but monophasic with [KCl] ≤ 0.1 mol/L. This suggests that, at high KCl concentrations, segments of the molecular chain are adjusted first and then the whole molecule undergoes rearrangement. We discuss the possible significance of these findings to an understanding of the way that spiders spin silk.

The outstanding mechanical properties (*1*) of the dragline silks of orb web spiders have prompted many investigations, and much is now known about the structure, function, and molecular chemistry of the threads (*2*). In comparison, remarkably little is known about the method of thread formation. However, this process involves a remarkable transition from a concentrated liquid crystalline solution (*3*−*6*) to a tough solid (*7*) with a preponderance of β-sheet secondary structure (*8*, *9*). The secondary structure of the protein before the transition may be a combination of random coil, α-helical, and β-turn (*10*) or simply random coil (*11*). A nucleation-dependent aggregation mechanism has been proposed on the basis of CD spectroscopy of *Bombyx* silk fibroin solutions (*12*). Mechanical strain produced by rapid extensional flow in the draw down process within the spider's spinning duct appears to be important in initiating the transition from liquid dope to solid thread (*13*). This phase transition is thought to be facilitated by a reduction in pH as the silk dope passes through the spinning duct (*14*−*16*). The addition of K^+ ion to dilute dope solutions produces a spontaneous formation of nanofibrils not induced by the same concentrations of Na^+, Ca^{2+}, or Mg^{2+} (*16*) while evidence from cryo-SEM-EDX suggests that the sodium ion concentration falls while the potassium ion concentration rises as the dope flows down the spinning duct (*15*). This suggests that changes in sodium and potassium ion concentrations may also have an effect on the transition.

Although several studies use spectroscopic methods to describe silk protein secondary structure in solutions, fibers, or films from spiders or silkworms (*10*, *17*−*20*), there has been little direct study of secondary structural transitions in spidroin or silkworm fibroin. CD spectroscopy has, however, been used to study the secondary structure transition induced by nucleation in *Bombyx* silk fibroin solutions (*12*) while transitions induced by ethanol in regenerated *Bombyx* fibroin films have been studied by time-resolved FTIR[1] spectroscopy (*21*). The latter technique provides a powerful method to examine protein conformation transitions on time scales as short as picoseconds (*22*−*24*).

In this paper, we report the use of time-resolved FTIR spectroscopy to investigate the conformation transition in *Nephila* spidroin film induced by the addition of potassium chloride solutions. The results presented here suggest that KCl can induce a conformation transition from random coil to β-sheet in spidroin films, but the transition is not as complete as that induced by alcohols. We discuss the possible significance of these findings to the spider's spinning mechanism.

MATERIALS AND METHODS

Preparation of Nephila Spidroin Film. The method is the same as described in our previous work (*16*): Final instar

† This work is supported by the British Biotechnology and Biological Sciences Research Council (BBSRC), the British Engineering and Physical Sciences Research Council (EPSRC), the Foundation for University Key Teachers by the Education Ministry of China, and the China/U.K. Science and Technology Cooperation Foundation as well as the National Natural Science Foundation of China (No. 29974005).

* Corresponding author: tel, +86-21-6564-2866; fax, +86-21-6564-0293; e-mail, chenx@fudan.edu.cn.

‡ Fudan University.

§ University of Oxford.

[1] Abbreviations: FTIR, Fourier transform infrared; KCl, potassium chloride; D_2O, deuterium oxide.

10.1021/bi026550m CCC: $22.00
Published on Web 11/20/2002

female *Nephila senegalensis* spiders were killed by crushing the cephalothorax and immediately dissected in spider Ringer (*25*) solution at pH 8.2. The ampulla (sac) of the major ampullate gland was transferred to fresh Ringer solution and the epithelium removed to expose the concentrated dope. Care was taken to avoid shearing this, as it is highly strain-sensitive when concentrated. The concentrated dope was gently blotted for 1 s on Kleenex paper and transferred to a tared plastic microcentrifuge tube. After reweighing, 100 μg of fresh deionized water was added per 2 mg of the blotted dope to give a dope concentration of 2 wt %. One milliliter of this solution was transferred to a 3 cm × 3 cm plastic weighing boat and allowed to dry overnight at approximately 25 °C and 50% relative humidity. The thickness of the film was approximately 5 μm.

FTIR Spectroscopy. We examined the FTIR spectra in the amide I region to define the secondary structures in *Nephila* spidroin films as prepared and after immersion in different KCl/D_2O solutions. All infrared spectra were recorded using a Nicolet Magna 550 FTIR spectrometer. To eliminate spectral contributions due to atmospheric water vapor, the instrument was continuously purged by dry air using a JUN-AIR OF302-25 compressor and a Peak Scientific P925L drying unit. The infrared spectra were recorded using a liquid nitrogen cooled MCT detector. For each measurement, 128 interferograms were coadded and Fourier transformed employing a Genzel-Happ apodization function to yield spectra with a nominal resolution of 4 cm^{-1}. For the preparation of time series, the interval between successive spectra in the rapid scan mode was 0.58 min.

The *Nephila* spidroin films were cut into 3 mm × 6 mm rectangular disks. For the time-resolved measurements, the *Nephila* spidroin film was placed between a pair of BaF_2 windows separated by a 100 μm spacer in a liquid cell. Solutions of potassium chloride dissolved in D_2O with concentrations ranging from 0.01 to 1.0 mol/L were then quickly injected into the liquid cell and the gathering spectra immediately initiated. Higher concentrations of KCl were not used as these can damage BaF_2 windows. Time series spectra were recorded for a period of 240 min using the parameters described above. Absorbance spectra at each time point were generated by dividing the single-beam spectrum collected at a specific time by a background spectrum and converting to absorbance using OMNIC 5.2 (Nicolet Instrument Corp.). Difference spectra were calculated by subtracting the absorbance spectrum recorded at 240 min from each absorbance spectrum collected at time *t* after addition of KCl solution. The data shown in the figures are from single experiments, but closely similar results were obtained in replicates. Kinetics of the KCl-induced conformation transition were studied by fitting curves using ORIGIN 5.0 (Microcal). The time constants from fitting curves to data for three separate runs were averaged and the means and standard deviations reported in Table 1. Peak separation of the amide I band was carried out using PeakFit 4.1 (SPSS Inc.). A Gaussian model was selected for the band shape; the band position was set at 1620, 1650, and 1691 cm^{-1}, respectively; and the bandwidth was autoadjusted by the software.

We also obtained spectra from dilute solutions of spidroin prepared by dissolving the contents of the major ampullate gland in D_2O overnight at room temperature as described above.

Table 1: Conformation Transition Kinetics of *Nephila* Spidroin Films Probed by Absorbance Changes of the β-Sheet Band at 1620 and 1691 cm^{-1} [a]

[KCl] (mol/L)	1620 cm^{-1}			1691 cm^{-1}		
	τ_1 (min)	τ_2 (min)	α_1 (%)	τ_1 (min)	τ_2 (min)	α_1 (%)
1.0	7.4 ± 2.4	53.3 ± 9.5	51 ± 7	7.8 ± 2.1	54.9 ± 6.2	43 ± 7
0.5	4.5 ± 2.5	49.8 ± 8.2	43 ± 9	4.0 ± 2.3	53.9 ± 2.2	33 ± 7
0.3	3.7 ± 0.2	48.6 ± 7.0	31 ± 5	3.0 ± 0.2	57.7 ± 5.9	21 ± 6

[KCl] (mol/L)	τ (min) at 1620 cm^{-1}	τ (min) at 1691 cm^{-1}
0.1	61.4 ± 7.3	69.4 ± 4.8
0.05	66.3 ± 7.0	70.7 ± 8.5
0.01	66.5 ± 6.1	72.5 ± 5.9

[a] The time constant, τ, and the amplitudes were obtained by the absorbance difference spectral amplitudes with exponential decay functions. The relative amplitudes α_1 were calculated by $\alpha_1 = A_1/(A_1 + A_2)$ (where A_1 and A_2 are the amplitudes of the first and the second phases, respectively).

RESULTS

Static FTIR Measurements of Nephila Spidroin Film. The amide I band for the dry untreated *Nephila* spidroin film showed a broad, slightly asymmetric envelope with a maximum at ~1660 cm^{-1} (see Figure 1a). A closely similar amide I band was seen in silkworm (*Bombyx mori*) fibroin films and has been attributed to a random coil and/or silk I structure (*21*, *26*−*28*). The shape of the amide I peak of *Nephila* spidroin films in D_2O was similar to that of the dry films, but the maximum shifted to 1647 cm^{-1}. Fresh spidroin dope dissolved in D_2O gave spectra almost identical to those of spidroin films in D_2O. According to the classic assignment of amide I bands (*29*−*31*), the peak around 1647 cm^{-1} in D_2O can be attributed to random coil conformation, the shift in absorption maximum in D_2O being common in proteins (*11*, *29*). However, some helical conformations, such as α-helix and 3_{10}-helix, have absorption bands similar to those of random coil (unordered structure) and are sometimes not well resolved; therefore, we assign the absorption peak around 1647 cm^{-1} to random coil and/or helical conformation in this study.

The amide I spectrum of dry spidroin film after immersion in 1.0 mol/L KCl solution for 24 h was quite complex with peaks at ~1656 and 1620 cm^{-1} as well as a shoulder around 1690 cm^{-1} (Figure 1b). The second derivative of the KCl-treated film revealed three components: sharp peaks at 1620 and 1693 cm^{-1} and a broad peak at 1655−1660 cm^{-1}. These peaks were assigned to β-sheets, high-frequency antiparallel β-sheets, and random coil and/or helical structures, respectively (*29*−*32*). The random coil and/or helical structure peak was significantly lower in KCl-treated films compared with untreated ones, suggesting partial conversion of random coil and/or helical structures to β-sheets.

Thus evidence from static observations on spidroin films suggests that ordered secondary structures may be formed from an initial disordered state.

Time-Resolved FTIR Measurement during the Conformation Transition Process of Nephila Spidroin Film Induced by 1.0 mol/L KCl/D_2O Solution. Figure 2a shows infrared spectra from 0.58 to 240 min after addition of 1.0 mol/L

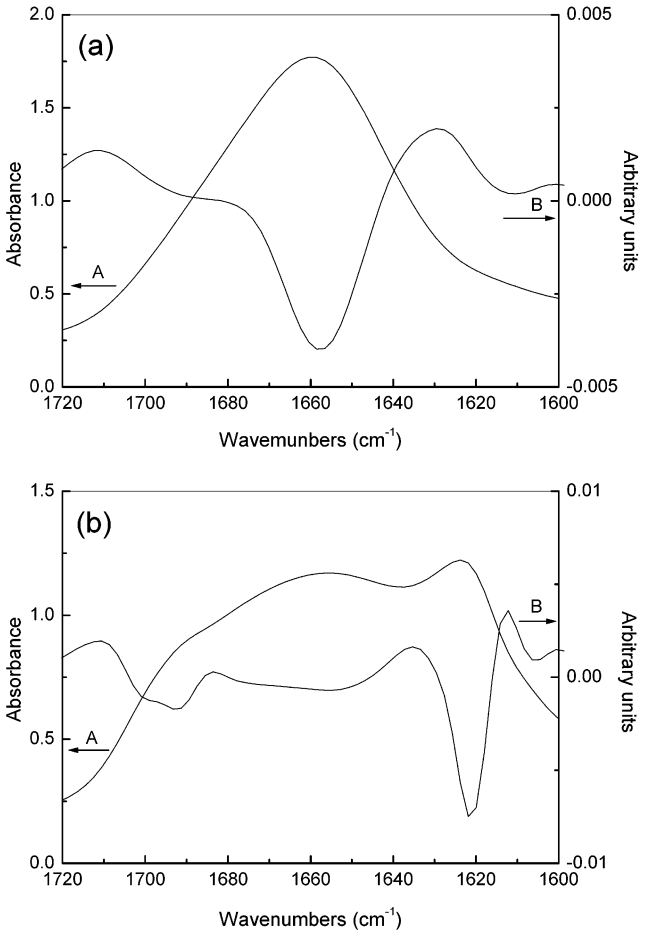

FIGURE 1: Amide I band of *Nephila* spidroin: (a) dry film without any treatment from casting; (b) film immersed in 1.0 mol/L KCl solution for 24 h and then dried (curve A, normal FTIR spectrum; curve B, second derivative spectrum).

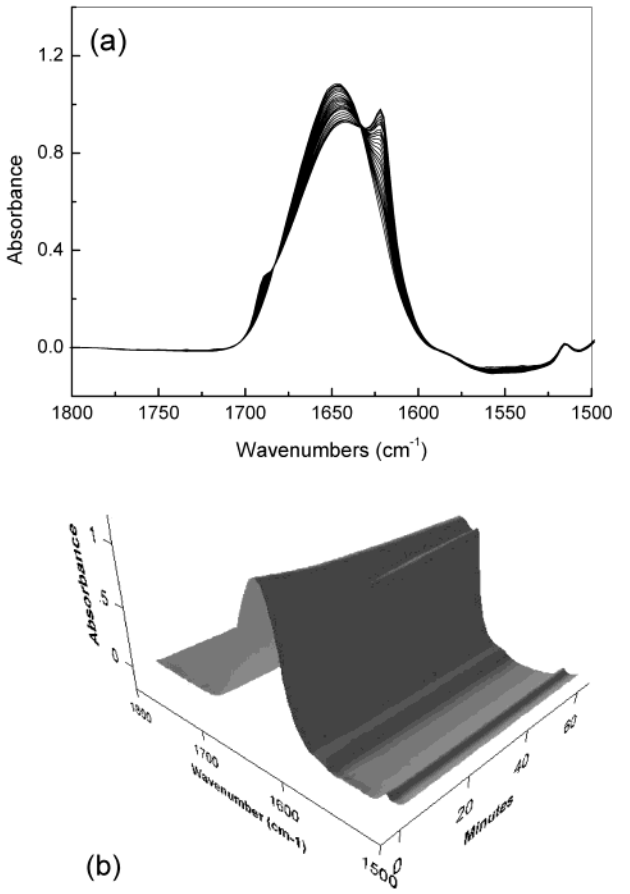

FIGURE 2: Original FTIR spectra of *Nephila* spidroin film during the conformation transition process from the beginning to 240 min: (a) normal spectra; (b) three-dimensional spectra.

KCl in D_2O to *Nephila* spidroin film. With increasing time, the amide I band gradually changed shape while the maximum shifted from ~1650 to ~1620 cm^{-1}. The changes can be examined more readily in difference spectra (Figure 3a) and visualized more clearly in three-dimensional plots (Figures 2b and 3b). The changes seen in the difference spectra in time series experiments are closely similar to those identified by second derivative analysis from static data (see Figure 1b). The increasing negative bands at 1620 and 1691 cm^{-1} reflected the increasing β-sheet structures while reduction in the single positive band around 1650 cm^{-1} indicated the loss of random coil and/or helical structures.

Intensity−time plots generated from difference spectra were used to study the kinetics of the formation of β-sheets (1620 cm^{-1}) and high-frequency antiparallel β-sheets (1691 cm^{-1}) (Figure 4a) and the loss of random coil and/or helical structures (1650 cm^{-1}) (Figure 4b) on addition of 1.0 mol/L KCl/D_2O solution to spidroin films. In all runs, the time−intensity plots of the formation of β-sheet and the loss of random coil and/or helical structures appeared coincident (Figure 4). Second-order (biphasic) exponential decay functions (eq 1) were fitted to the intensity−time plots:

$$A = A_1 \exp(-t/\tau_1) + A_2 \exp(-t/\tau_2) \qquad (1)$$

where A denotes the Δabsorption in difference spectra; t denotes the experiment time; and τ_1, τ_2, A_1, A_2 are the time constants and amplitudes of the first and the second phases, respectively.

The first (τ_1) and second (τ_2) time constants describing the formation of β-sheet (7.4 ± 2.4 and 53.3 ± 9.5 min) and high-frequency antiparallel β-sheet (7.8 ± 2.1 and 54.9 ± 6.2 min) and the disappearance of random coil and/or helical structures (8.5 ± 1.7 and 55.3 ± 7.0 min) were closely similar in all three cases. Thus, the time constants for the disappearance of random coil and/or helical structures coincided with those for the appearance of β-sheet when allowance is made for experimental error. The coincident nature of all three time−intensity plots and similarity of the time constants indicate a rather simple conversion of random coil and/or helical structures into β-sheet.

Influence of KCl Concentration on the Conformation Transition Kinetics of Nephila Spidroin Films. Figure 5 shows the effect of the concentration of KCl in D_2O applied to the spidroin films on the last spectra (240 min) in time series experiments. With increase in KCl concentration, the peak around 1620 cm^{-1} (β-sheet) increased. Figure 6 shows that the β-sheet content in the film determined by peak fitting increased with increasing KCl concentration.

Figure 7 shows the normalized Δabsorbance vs time curves of the films in different concentrations of KCl solutions in order to compare the conformation transition kinetics. It clearly shows that the rate of formation of β-sheet increased with the increase of KCl concentration. The experimental data could be fitted with second-order exponential functions for [KCl] ≥ 0.3 mol/L, but the functions changed to first-

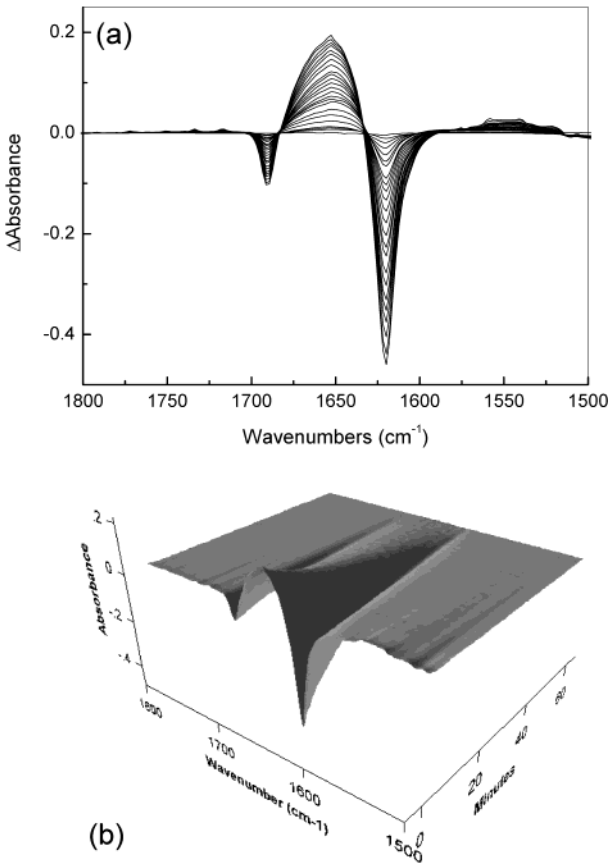

FIGURE 3: Difference FTIR spectra of *Nephila* spidroin film during the conformation transition process from the beginning to 240 min: (a) normal spectra; (b) three-dimensional spectra.

order exponential functions for [KCl] ≤ 0.1 mol/L. Table 1 shows the effect of different KCl concentrations on the conformation transition time constants obtained by fitting these functions. With increase in KCl concentration from 0.3 to 1.0 mol/L, although the time constant of the faster phase (τ_1) lengthened (e.g., from 3.7 to 7.4 min for β-sheet formation), the percentage of the faster phase (see Table 1) also increased significantly (from 31% to 51% for β-sheet formation). Therefore, despite this lengthening of the time constant, there was still an increase of the transition rate with increase in KCl concentration. When [KCl] ≤ 0.1 mol/L, the fit functions were first-order exponentials in which the fast phase was missing compared to the transition in the more concentrated KCl solutions, and this resulted in a slow transition rate.

DISCUSSION

Assignment of the 1691 cm^{-1} Peak in FTIR Spectra of Nephila Spidroin Films. The infrared peak around 1691 cm^{-1} in the amide I band always appears alongside the β-sheet peak (~1620 cm^{-1}) (*11*, *33*−*36*). In the early studies of silk protein conformation, this peak was assigned to β-sheets (*11*, *34*) or simply neglected (*33*, *35*). On the basis of the classical assignment, the 1691 cm^{-1} band is assigned to the high-frequency band of the antiparallel β-sheet structure. However, it has been reported that this band may also be assigned to turns and/or bends (*36*, *37*). Therefore, we think the 1691 cm^{-1} band may be attributed to the antiparallel β-sheet structure and the turns or bends associated to this antiparallel

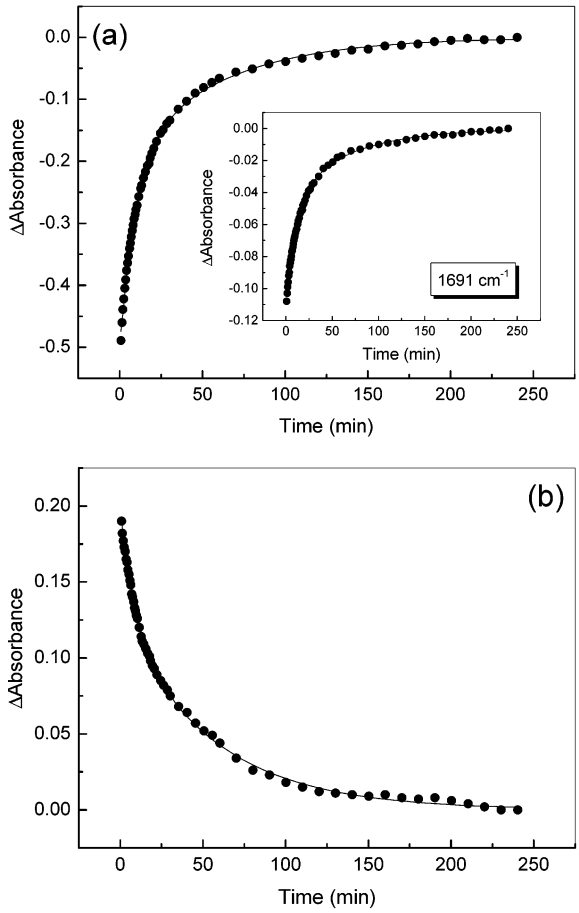

FIGURE 4: Conformation transition kinetics of *Nephila* spidroin film monitored by time-resolved FTIR spectroscopy: (a) increase of β-sheet at 1620 and 1691 cm^{-1}; (b) decrease of random coil and/or helical structures around 1650 cm^{-1}.

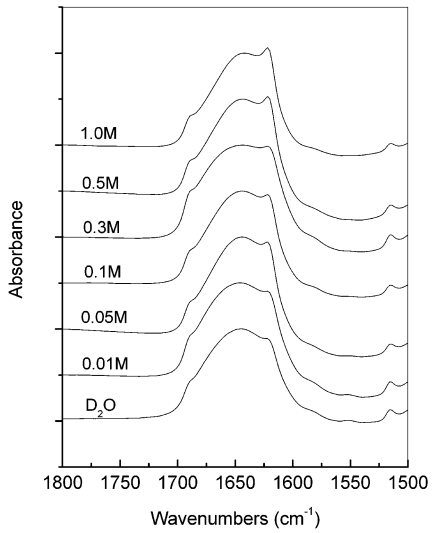

FIGURE 5: The last spectra (240 min) of *Nephila* spidroin films during the dynamic measurements recorded at different KCl concentrations.

β-sheet structure. This is supported by the observations presented above that the kinetics for the formation of the 1620 and 1691 cm^{-1} bands (Table 1) were consistently different at [KCl] ≥ 0.3 mol/L as follows. Although the time constants of the 1620 and 1691 cm^{-1} bands were the same within experimental error, the percentage of the fast phase (α_1) of the 1620 cm^{-1} band is regularly about 10% larger

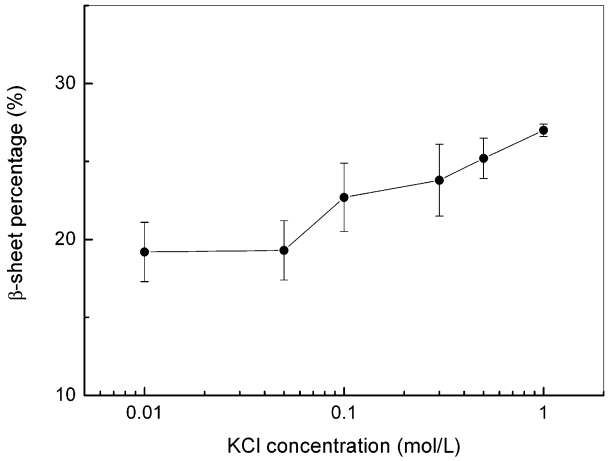

FIGURE 6: β-Sheet content of *Nephila* spidroin films after the conformation transition process at different KCl concentrations.

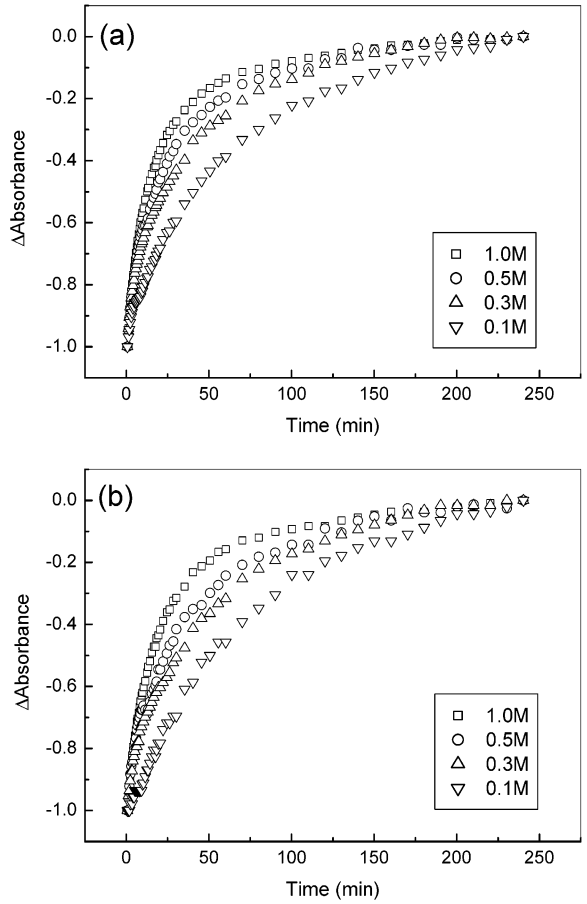

FIGURE 7: Comparison of conformation transition kinetics of *Nephila* spidroin films induced by different concentrations of KCl: (a) band at 1620 cm^{-1}; (b) band at 1691 cm^{-1}.

than the 1691 cm^{-1} band (which means there is a greater contribution from the fast phase resulting in a faster transition rate for the formation of the 1620 cm^{-1} band compared to the 1691 cm^{-1} band). We have found a similar phenomenon in our previous work using ethanol to induce a conformation transition in silk fibroin (*21*).

Further support for the hypothesis that turns and/or bends form at the same time but not necessarily at the same rate as β-sheets comes from a consideration of the nature of the antiparallel β-sheet structure. Ample evidence has accumulated that this arrangement predominates in both spider and silkworm silk threads (*8*, *38*, *39*). The enormous energy requirement to fully extend the very long molecules of spidroin and fibroin [the molecular masses are 275−320 and 300−360 kDa, respectively (*21*, *40*)] and the difficulty of ensuring that alternate molecules run in opposite directions rule out the possibility that antiparallel β-sheets are formed by laying single extended macromolecular chains together. It is therefore reasonable, however, to assume that the macromolecular chains are repeatedly folded back on themselves and therefore give rise to turns or bends and that the kinetics for the formation of these structures need not be identical to the kinetics for the formation of β-sheets. We emphasize that although we have insufficient evidence to show conclusively that the 1691 cm^{-1} band should be assigned to turns and bends, we suggest that these structures may contribute to this band.

Mechanism of the Conformation Transition. Evidence above indicates that addition of potassium chloride to spidroin films induces a transition from random coil and/or helical structures to β-sheet. This is of considerable interest in view of the evidence from cryo-SEM-EDX that indicates that the concentration of potassium ions increases as the protein dope passes down the spider's spinning duct (*15*) and evidence we have presented earlier (*16*) that adding potassium ions to dilute spider dope solutions rather specifically induces a spontaneous formation of nanofibrils. Taken together, these lines of evidence support the hypothesis that potassium ions play a part in the natural spinning process by facilitating the formation of β-sheets in spidroin and hence initiating the formation of nanofibrils. A similar effect may occur in *Bombyx* silkworms as the potassium ion concentration is also thought to increase as fibroin flows through the secretory pathway (*41*).

We have argued above that the conformation transition induced in spidroin by potassium chloride may not require an ordered secondary structure as a starting point. In addition, the NMR data of *Nephila* spidroin in solution (*10*) indicate a strong preponderance of random coil conformation (see also ref *42*). Putting this together with our observation reported above that the absorption wavenumber of amide I was practically identical for spidroin solution and spidroin film, it strongly supports the suggestion that both film and solution have mainly random coil conformation. This has the advantage of presenting a relatively low energy barrier to the transition as here energy is mainly required only to break and re-form hydrogen bonds and not to fully extend or radically refold protein chains.

A range of factors induces a transition from random coil and/or helical structures to β-sheet in spidroin and fibroin in addition to the effect of potassium chloride described above. These include organic solvents with a high dielectric constant (methanol, ethanol, dioxane, etc.), mechanical treatment, heating or cooling, and blending with other polymers (*21*). Of these, only mechanical strain and the addition of potassium ions could be considered to be physiological though a small increase in temperature is conceivable as the natural spinning processes may not be isothermal.

The transition rate in silkworm fibroin films treated with ethanol (*21*) ($\tau_1 = 0.56$ min; $\tau_2 = 5.20$ min) is much quicker than that in spidroin films treated with KCl ($\tau_1 = 7.4$ min; $\tau_2 = 53.3$ min). The slower kinetics in the latter has the

advantage of making it easy to study the early events in the transition. Kinetics this slow would imply that the transition needs to be initiated well before the dope reaches the rapid internal draw down process (*4*) in vivo and might explain why the maximum spinning speed in spiders is so slow compared with industrial spinning methods (*13*). Caution must be exercised in extrapolating from in vitro experiments to in vivo spinning as conditions in the living spider (low pH and concentrated aqueous spinning solutions) are different from those in the present study (films cast from dilute solutions of spidroin and immersed in D_2O). However, both in vivo and in vitro systems are highly hydrated; the spidroin spinning dope taken from the gland contains approximately 65% water (*16*) while silk protein films contain approximately 30% water when swollen (*43*).

The spidroin/KCl transition (at KCl concentrations above 0.1 mol/L) showed a remarkable resemblance to the fibroin/ethanol transition (*21*) in that both are described by second-order exponential functions. This suggests that the mechanism of hydrogen bond rupture in spidroin treated with KCl may be similar to that in fibroin treated with ethanol but slower. Bond rupture and the resulting swelling of the films in both instances may allow the polymer chains to move more freely to allow new β-sheet hydrogen bonds to form. It is well-known that spidroin contains poly(Ala)$_n$ segments in which $n = 4-9$, while Ober et al. (*44*) found that relatively short lengths ($n = 5-10$) of poly(Ala)$_n$ prefer a β-sheet conformation. Therefore, under favorable conditions the spidroin macromolecules have a strong preference for a β-sheet structure. The fast phase of the transition (τ_1) may represent an initial formation of β-sheets arising from the adjustment of individual segments of spidroin molecules within films. This is compatible with evidence suggesting that conformation transitions of polymers in general occur initially by local distortion of nearby parts of the molecule and do not require gross movements of the macromolecule (*45*). After the initial rapid rearrangement of segments, the remaining potential β-sheet-forming domains may not be favorably positioned to form hydrogen bonds without a slow intermolecular rearrangement. We suggest that the latter takes place during the second, slow phase described by τ_2. Potassium ion has a stronger chaotropic effect than sodium ion (*16*), giving them a somewhat selective and concentration-dependent ability to weaken hydrogen bonds, so a [KCl]-dependent increase in mobility of chains may account for the shortening of τ_2 values with increase in KCl concentration and the appearance of τ_1 at a critical concentration in excess of 0.1 mol/L.

While we recognize that structural transitions in spidroin films cast from dilute solutions and studied in the D_2O required for FTIR spectroscopy may be different from those in concentrated spidroin solutions in light water, our results give insight into the kinetics of an interesting transition in this remarkable protein.

Finally, the conformation transition in spidroin films induced by potassium chloride may prove a useful model for the study of random coil and/or helical structures to β-sheet transitions in other proteins. In this connection it is interesting to note that spidroin shows a marked similarity to amyloidogenic proteins (*46*).

ACKNOWLEDGMENT

We thank Prof. Tongyin Yu and Dr. Ping Zhou at Fudan University for helpful advice and discussion and Mr. Paul Embden at the University of Oxford for assistance with the spiders. Further discussion was facilitated by the ESF through their SILK network.

REFERENCES

1. Gosline, J. M., Denny, M. W., and DeMont, M. E. (1984) Spider silk as rubber, *Nature 309*, 551−552.
2. Vollrath, F., and Knight, D. P. (2001) Liquid crystalline spinning of spider silk, *Nature 410*, 541−548.
3. Viney, C. (1997) Natural silks: Archetypal supramolecular assembly of polymer fibres, *Supramol. Sci. 4*, 75−81.
4. Knight, D. P., and Vollrath, F. (1999) Liquid crystals and flow elongation in a spider's silk production line, *Proc. R. Soc. London, Ser. B 266*, 519−523.
5. Kerkam, K., Viney, C., Kaplan, D., and Lombardi, S. (1991) Liquid crystallinity of natural silk secretions, *Nature 349*, 596−598.
6. Willcox, P. J., Gido, S. P., Muller, W., and Kaplan, D. L. (1996) Evidence of a cholesteric liquid crystalline phase in natural silk spinning processes, *Macromolecules 29*, 5106−5110.
7. Knight, D. P., Knight, M. M., and Vollrath, F. (2000) Beta transition and stress-induced phase separation in the spinning of spider dragline silk, *Int. J. Biol. Macromol. 27*, 205−210.
8. Riekel, C., Branden, C., Craig, C., Ferrero, C., Heidelbach, F., and Muller, M. (1999) Aspects of X-ray diffraction on single spider fibers, *Int. J. Biol. Macromol. 24*, 179−186.
9. Kummerlen, J., vanBeek, J. D., Vollrath, F., Meier, B. H. (1996) Local structure in spider dragline silk investigated by two-dimensional spin-diffusion nuclear magnetic resonance, *Macromolecules 29*, 2920−2928.
10. Hijirida, D. H., Do, K. G., Michal, C., Wong, S., Zax, D., and Jelinski, L. W. (1996) C-13 NMR of *Nephila clavipes* major ampullate silk gland, *Biophys. J. 71*, 3442−3447.
11. Venyaminov, S. Y., and Kalnin, N. N. (1990) Quantitative IR spectrophotometry of peptide compounds in water (H_2O) solutions. 2. Amide absorption-bands of polypeptides and fibrous proteins in alpha-coil, beta-coil, and random coil conformations, *Biopolymers 30*, 1259−1271.
12. Li, G. Y., Zhou, P., Shao, Z. Z., Xie, X., Chen, X., Wang, H. H., Chunyu, L. J., and Yu, T. Y. (2001) The natural silk spinning process−A nucleation-dependent aggregation mechanism, *Eur. J. Biochem. 268*, 6600−6606.
13. Knight, D. P., and Vollrath, F. (2001) Comparison of the spinning of Selachian egg case ply sheets and orb web spider dragline filaments, *Biomacromolecules 2*, 323−334.
14. Barghout, J. Y. J., Czernuszka, J. T., and Viney, C. (2001) Multiaxial anisotropy of spider (*Araneus diadematus*) cocoon silk fibres, *Polymer 42*, 5797−5800.
15. Knight, D. P., and Vollrath, F. (2001) Changes in element composition along the spinning duct in a *Nephila* spider, *Naturwissenschaften 88*, 179−182.
16. Chen, X., Knight, D. P., and Vollrath, F. (2002) Rheological characterization of *Nephila* spidroin solution, *Biomacromolecules 3*, 644−648.
17. Lenormant, H. (1955) Infrared spectra and structure of the proteins of the silk glands, *Trans. Faraday Soc. 52*, 549−553.
18. Shao, Z., Vollrath, F., Sirichaisit, J., and Young, R. J. (1999) Analysis of spider silk in native and supercontracted states using Raman spectroscopy, *Polymer 40*, 2493−2500.
19. Shao, Z. Z., Young, R. J., and Vollrath, F. (1999) The effect of solvents on spider silk studied by mechanical testing and single-fibre Raman spectroscopy, *Int. J. Biol. Macromol. 24*, 295−300.
20. Chen, X., Li, W. J., and Yu, T. Y. (1997) Conformation transition of silk fibroin induced by blending chitosan, *J. Polym. Sci., Part B: Polym. Phys. 35*, 2293−2296.
21. Chen, X., Shao, Z. Z., Marinkovic, N. S., Miller, L. M., Zhou, P., and Chance, M. R. (2001) Conformation transition kinetics of regenerated *Bombyx mori* silk fibroin membrane monitored by time-resolved FTIR spectroscopy, *Biophys. Chem. 89*, 25−34.
22. Reinstadler, D., Fabian, H., Backmann, J., and Naumann, D. (1996) Refolding of thermally and urea-denatured ribonuclease a monitored by time-resolved FTIR spectroscopy, *Biochemistry 35*, 15822−15830.

23. Williams, S., Causgrove, T. P., Gilmanshin, R., Fang, K. S., Callender, R. H., Woodruff, W. H., and Dyer, R. B. (1996) Fast events in protein folding: helix melting and formation in a small peptide, *Biochemistry 35*, 691−697.
24. Gilmanshin, R., Williams, S., Callender, R. H., Woodruff, W. H., and Dyer, R. B. (1997) Fast events in protein folding: relaxation dynamics and structure of the I form of apomyoglobin, *Biochemistry 36*, 15006−15012.
25. Schartau, W., and Leidescher, T. (1983) Composition of the Hemolymph of the *Tarantula Eurypelma*−Californicum, *J. Comput. Physiol. 152*, 73−77.
26. Magoshi, J., Mizuide, M., Magoshi, Y., Takahashi, K., Kubo, M., and Nakamura, S. (1979) Physical properties and structure of silk. VI. Conformational changes in silk fibroin induced by immersion in water at 2 and 130 °C, *J. Polym. Sci., Polym. Phys. Ed. 17*, 515−520.
27. Asakura, T., Kuzuhara, A., Tabeta, R., and Saito, H. (1985) Conformation characterization of *Bombyx-mori* silk fibroin in the solid-state by high-frequency C-13 cross polarization magic angle spinning NMR, X-ray-diffraction, and infrared-spectroscopy, *Macromolecules 18*, 1841−1845.
28. Freddi, G., Romano, M., Massafra, M. R., and Tsukada, M. (1995) Silk fibroin/cellulose blend films−preparation, structure, and physical-properties, *J. Appl. Polym. Sci. 56*, 1537−1545.
29. Byler, D. M., and Susi, H. (1986) Examination of the secondary structure of protein by deconvolved FTIR spectra, *Biopolymers 25*, 469−487.
30. Surewicz, W. K., and Mantsch, H. H. (1988) New insight into protein secondary structure from resolution-enhanced infrared-spectra, *Biochim. Biophys. Acta 952*, 115−130.
31. Dong, A., Huang, P., and Caughey, W. S. (1990) Protein secondary structures in water from 2nd-derivative amide-I infrared-spectra, *Biochemistry 29*, 3303−3308.
32. Simonetti, M., and Di Bello, C. (2001) New Fourier transform infrared based computational method for peptide secondary structure determination. I. Description of method, *Biopolymers 62*, 95−108.
33. Yoshimizu, H., and Asakura, T. (1990) The structure of *Bombyx-mori* silk fibroin membrane swollen by water studied with ESR, C-13-NMR, and FT-IR spectroscopies, *J. Appl. Polym. Sci. 40*, 1745−1756.
34. Ayub, Z. H., Arai, M., and Hirabayashi, K. (1994) Quantitative structural-analysis and physical-properties of silk fibroin hydrogels, *Polymer 35*, 2197−2200.
35. Freddi, G., Monti, P., Nagura, M., Gotoh, Y., and Tsukada, M. (1997) Structure and molecular conformation of tussah silk fibroin films: effect of heat treatment, *J. Polym. Sci., Part B: Polym. Phys. 35*, 841−847.
36. Khurana, R., and Fink, A. L. (2000) Do parallel beta-helix proteins have a unique Fourier transform infrared spectrum, *Biophys. J. 78*, 994−1000.
37. Tretinnikov, O. N., and Tamada, Y. (2001) Influence of casting temperature on the near-surface structure and wettability of cast silk fibroin films, *Langmuir 17*, 7406−7413.
38. Seidel, A., Liivak, O., and Jelinski, L. W. (1998) Artificial spinning of spider silk, *Macromolecules 31*, 6733−6736.
39. Asakura, T., Ashida, J., Yamane, T., Kameda, T., Nakazawa, Y., Ohgo, K., and Komatsu, K. (2001) A repeated beta-turn structure in poly(Ala-Gly) as a model for silk I of *Bombyx mori* silk fibroin studied with two-dimensional spin-diffusion NMR under off magic angle spinning and rotational echo double resonance, *J. Mol. Biol. 306*, 291−305.
40. Kaplan, D., Adams, W. W., Farmer, B., and Viney, C. (1994) Silk−biology, structure, properties, and genetics, *ACS Symp. Ser. 544*, 2−16.
41. Magoshi, J., Magoshi, Y., and Nakamura S. (1994) Mechanism of fiber formation of silkworm, *ACS Symp. Ser. 544*, 292−310.
42. Liivak, O., Flores, A., Lewis, R., and Jelinski, L. W. (1997) Conformation of the polyalanine repeats in minor ampullate gland silk of spider *Nephila clavipes*, *Macromolecules 30*, 7127−7130.
43. Chen, X., Li, W. J., Zhong, W., Lu, Y. H., and Yu, T. Y. (1998) Studies on chitosan-fibroin blend membranes (I)−Structure of the blend membrane and the improvement of the water adsorption and the mechanical property of fibroin, *Chem. J. Chin. Univ. 19*, 300−304.
44. Delvin, A., Ober, C. K., and Bluhm, T. L. (1989) Fourier transform Raman studies of secondary structure in synthetic polypeptides, *Macromolecules 22*, 500−502.
45. Helfand, E. (1984) Dynamics of conformational transitions in polymers, *Science 226*, 647−650.
46. Kenney, J. M., Knight D. P., Wise, M. J., and Vollrath, F. (2002) Amyloidogenic nature of spider silk, *Nature* (in press).

BI026550M